MRI in Head and Neck Radiotherapy Planning

Houda Bahig, M.D.[1]; Karim Boudam, Ph.D.[1]; David Landry, M.D.[2]; Edith Filion, M.D.[1]; Olivier Ballivy, M.D.[1]; David Roberge, M.D.[1]; Jean-Charles Côté, Ph.D.[1]; Phuc-Félix Nguyen-Tan, M.D.[1]

[1] Department of Radiation Oncology, Centre Hospitalier de l'Université de Montréal, Montreal, Quebec, Canada
[2] Department of Radiology, Centre Hospitalier de l'Université de Montréal, Montreal, Quebec, Canada

The introduction of intensity modulated radiotherapy (IMRT) as standard of care as well as the sustained improvements in image-guidance have significantly increased the precision and complexity of head and neck cancer (HNC) radiotherapy (RT) planning. As have many other institutions, the Centre Hospitalier de l'Université de Montréal (CHUM), a high-volume center for head and neck oncology, has adopted a multi-modality imaging approach for RT planning in locally advanced HNC. This approach includes routine acquisition of fluorodeoxyglucose-positron emission tomography (FDG-PET) and magnetic resonance imaging (MRI) using RT-dedicated technologies, combined with contrast-enhanced planning computed tomography (CT). While the use of IMRT allows for improved conformity of dose distribution, it requires accurate tumor volume definition in order to prevent target-miss or unnecessary dose to organs at risk. In this report, we describe CHUM's planning MRI workflow for locally advanced HNC and we discuss the current role of MRI in HNC planning.

MRI in head and neck cancer – planning workflow at CHUM

The current approach at CHUM involves the systematic acquisition of a planning CT for dose calculation, as well as MRI sequences in treatment position for improvement of soft-tissue delineation and optimal registration with planning CT for HNC cases. This is of particular importance in HNC where differences in imaging planes and neck flexion

Figure 1: T2-weighted MRI allows to detect a base of tongue lesion that is occult on CT scan.

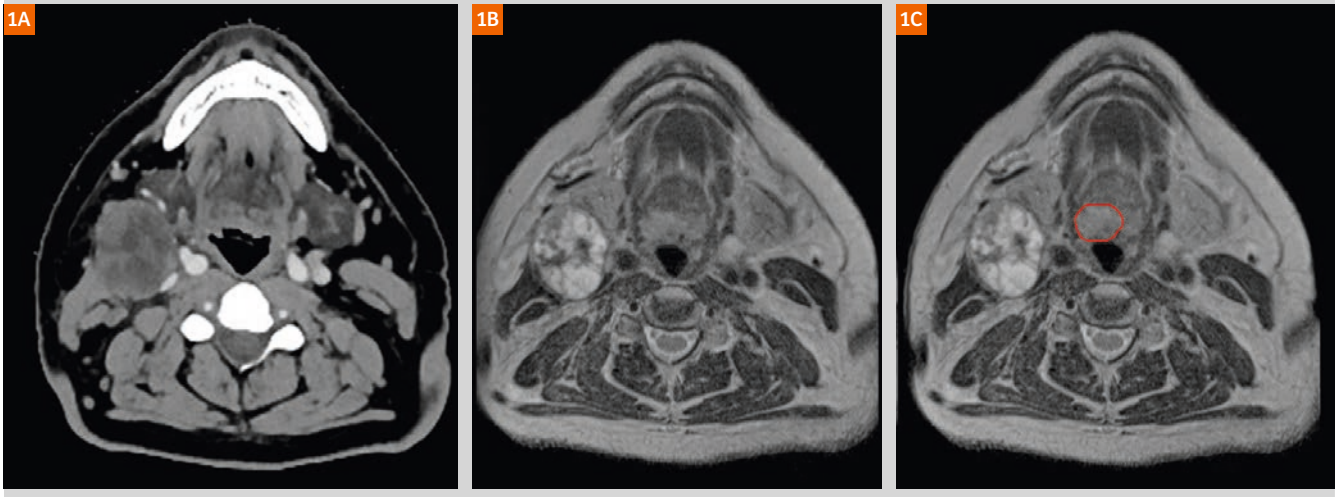

This patient presented with a right T1N2b squamous cell cancer of the base of tongue. **(1A)** Planning contrast-enhanced CT scan shows a large level IIA necrotic lymph node but fails to detect primary tumor; **(1B, C)** axial T2-weighted MRI sequence shows a suspicious hyper-intensity at the right base of tongue measuring 1.6 x 1.3 cm and corresponding to the known primary tumor detected on fiberoptic nasopharyngoscopy.

between planning and diagnostic imaging can be major. MRI planning examinations are obtained on a RT-dedicated 70 cm open bore 1.5 Tesla system (MAGNETOM Aera, Siemens Healthcare, Erlangen, Germany). The images are acquired in treatment position with a head and neck thermoplastic mask fixed to a custom hard foam flat table insert. Due to the incompatibility between the head and neck mask and the standard head coil, surface radiofrequency coils are used [1]; this typically involves a spine array coil posteriorly and a large 18-channel flexible array coil anteriorly (Siemens Healthcare, Erlangen, Germany).

Our institutional planning MRI protocols have been adapted to RT planning through optimization of resolution and geometric distortions, resulting in scanning parameters that differ from those used in diagnostic radiology. All sequences were corrected for geometric distortion using the built in 3D correction algorithm. Parameters of the sequences currently used in our standard workflow are as follows:

(1) **Transverse T2-weighted Turbo Spin Echo (TSE) sequence:** Repetition time (TR) / echo time (TE) 5610/80 ms, field-of-view (FOV) 19 cm, voxel resolution 0.6 mm x 0.6 mm x 3.0 mm, matrix 224 x 320 and bandwidth 191 Hz/pixel. In patients presenting dental restorations, a modified metallic artifact protocol is used, with the following parameters: TR/TE 5000/91 ms, FOV 20 cm, voxel resolution 0.6 x 0.6 x 2.0 mm, matrix 320 x 320 and bandwidth 488 Hz/pixel.

(2) **Transverse T1-weighted TSE sequence:** TR/TE 689/23 ms, FOV 19 cm, voxel resolution 0.6 x 0.6 x 3.0 mm, matrix 224 x 320, bandwidth 200 Hz/pixel. Parameters of the modified metallic artifact protocol: TR/TE 626/9 ms, FOV 20 cm, voxel resolution 0.6 x 0.6 x 2.0 mm, matrix 320 x 320, and bandwidth 504 Hz/pixel.

(3) **Transverse post-gadolinium T1-weighted fat saturated TSE sequence:** TR/TE 739/23 ms, FOV 19 cm, voxel resolution 0.6 x 0.6 x 3.0 mm, matrix 224 x 320, bandwidth 200 Hz/pixel. Parameters of the modified metallic artifact protocol: TR/TE 654/9 ms, FOV 20 cm, voxel resolution 0.6 x 0.6 x 2.0 mm, matrix 320 x 320 and bandwidth 504 Hz/pixel.

In addition to anatomic sequences, a focused diffusion-weighted sequence targeting gross tumor volume (GTV) is also routinely obtained before gadolinium injection, using a transverse short tau inversion recovery-echo planar imaging (STIR EPI) sequence with the following parameters: TR/TE 6900/81 ms, FOV 26 cm, voxel resolution 2.0 x 2.0 x 5.0 mm, matrix 119 x 128, bandwidth 1302 Hz/pixel. Three b-values are applied: 0, 500, 1000 s/mm^2, with diffusion gradient encoding in 3 orthogonal directions and combined into a trace image.

After their acquisition, MRI sequences are co-registered with the planning CT. Primary and nodal GTV delineation is performed using multimodality information from contrast and non-contrast CT, MRI as well as FDG-PET. Our institutional protocol involves systematic formal interpretation of MRI imaging of all patients by an expert head and neck radiologist.

Advantages of MRI in HNC planning

MRI is now routinely integrated in the HNC RT planning workflow [2, 3]. While planning CT provides the geometric integrity and relative electron density crucial for dose calculation, MRI co-registration to the planning CT has become indispensable for precise contouring in HNC owing to the improved soft tissue contrast. The use of an RT dedicated MRI has the advantage of increasing accessibility and allowing optimal scheduling within radiation oncology, without encroaching on diagnostic time slots. In addition, our 70 cm open bore RT MRI allows for acquisition of images in treatment position with immobilisation devices in place. For optimal RT planning imaging, major particularities of an RT dedicated MRI system include use of: (a) adapted planning MRI acquisition protocols, (b) compatible immobilisation devices, (c) flat table tops, and (d) surface coils rather than standard MRI head coils [4–6]. In addition, when looking forward to MR-only planning, in-room mobile lasers may be required. Use of planning MRI in HNC was shown to increase the precision of CT-to-MR registration compared to use of diagnostic MRI [7, 8]. In a study including 22 patients with oropharyngeal cancer, Hanvey et al. showed that MRI in treatment position was associated with a reduction of mean geometric error from 7 mm to 2 mm which translated in significant improvement of dose distribution [8]; data on the clinical impact of this improvement is still needed.

The excellent soft-tissue contrast of MRI is of particular importance in HNC where discrimination between tumor and surrounding healthy tissues is as challenging as it is crucial to avoid unnecessary dose to organs at risk. MRI has been associated with increased accuracy of GTV definition in oral cavity, oropharynx, and nasopharynx [9, 10]. In addition, MRI multi-planar imaging helps cranio-caudal tumor delimitation [11–14]. Importantly, use of morphological MRI in RT planning has been associated with reduced inter-observer variability for both GTV and organs at risk contouring [7, 12, 15]. In a prospective study of 10 patients with oropharynx cancer using multimodality assessment based on MRI, FDG-PET, and CT – MRI had the lowest inter-observer variability [16]; this is critical as delineation variability was shown to have a large impact on dose to both tumor and organs at risk [17]. International head and neck consensus guidelines, published in 2015, strongly recommend the use of MRI for RT planning for oral cavity, oropharynx, and nasopharynx tumors, as well as for delineation of several organs at risk (brainstem, spinal cord, pituitary gland, lacrimal glands, optic structures, parotid glands, and pharyngeal constrictor muscles) [18]. Precise MRI-based delineation of organs at risk is particularly useful when the GTV is in the vicinity of critical structures. Figure 1 shows an example of a patient with stage T1N2b squamous cell carcinoma of the base of tongue who

presented a radio-graphically occult primary tumor on contrast-injected CT. This tumor was however detected on a T2-weighted MRI as a suspicious heterogeneous signal. Figure 2 shows an example of a large T4aN2c squamous cell cancer of the base of tongue with anterior extension to the extrinsic muscles of tongue. As can be observed, the limits of the tumor are better defined on MRI.

The advantage of MRI for delineation of nodal disease is more controversial [19, 20]. Anatomical MRI may however offer an advantage in the particular context of retropharyngeal lymph nodes. In a study comparing the diagnostic accuracy of CT versus MRI for detection of metastatic retropharyngeal lymph nodes in 38 patients with nasopharynx or oropharynx cancers, the two modalities were found to have similar specificity but

Figure 2: MRI improving delineation of a base of tongue tumor.

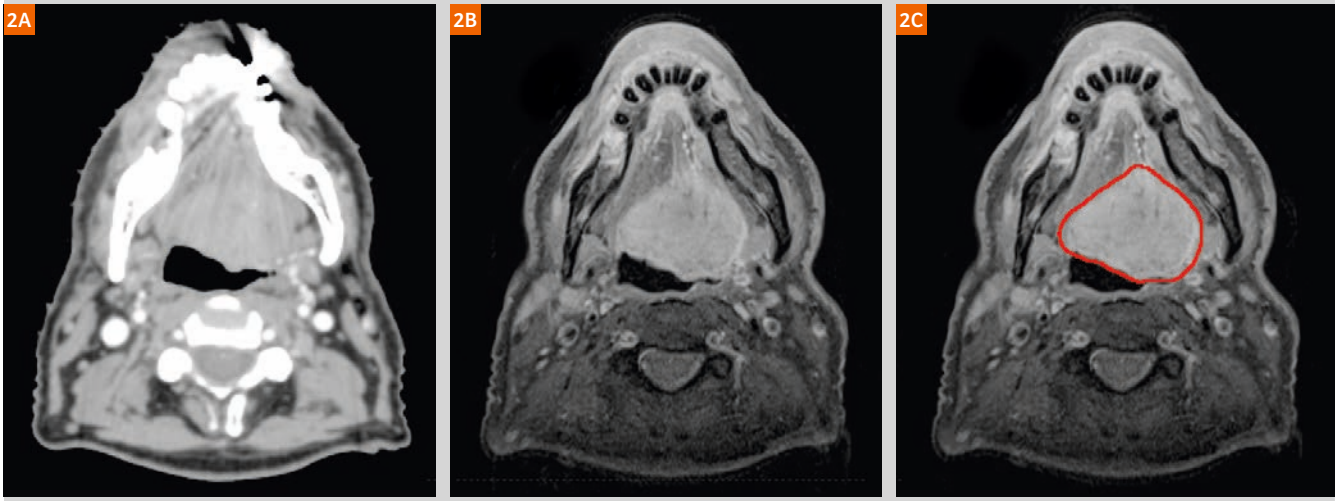

This patient presented with a left T4aN2c squamous cell cancer of the base of tongue. **(2A)** Planning contrast-enhanced CT scan shows a large base of tongue mass; **(2B, C)** axial contrast-injected T1-weighted MRI sequence shows a large 5.4 cm base of tongue lesion with anterior extension to the extrinsic muscles of the tongue; anterior, lateral and posterior limits of the tumor are better appreciated on MRI.

Figure 3: MRI improving detection and delineation of retropharyngeal lymph nodes.

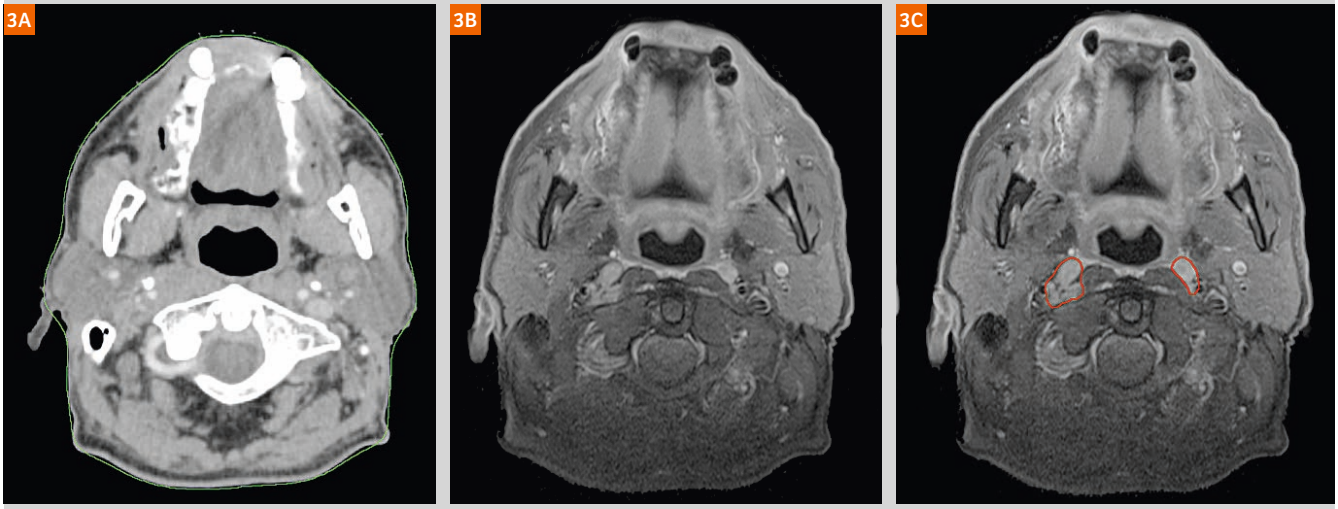

This patient presented with a T2N2c squamous cell cancer of the oropharynx. While bilateral retropharyngeal lymph nodes are suspected on contrast-injected CT scan **(3A)**, gadolinium-enhanced T1-weighted MRI allows better visualisation and delineation of bilateral retropharyngeal lymph nodes **(3B, C)**.

MRI had a superior sensitivity [21]. Figure 3 shows the example of a patient presenting with a T2N2c squamous cell cancer of the oropharynx with bilateral retropharyngeal lymphadenopathies, better observed on gadolinium-enhanced T1-weighted MRI sequence.

The advantage of MRI in HNC RT planning is perhaps most eloquent in the context of base of skull tumors, where the use of MRI has been associated with not only decreased inter-observer variation [22], but also increased identification of intracranial and perineural spreads which are poorly visualized on CT scan [22–24]. In a study by Chung et al. [9] involving 258 patients with nasopharyngeal carcinoma, MRI had significantly higher detection rate of intracranial and pterygo-palatine fossa infiltrations compared to CT, which translated into both improved tumor delineation and staging. In addition, although bone cortex erosion is often better appreciated on CT, MRI may be superior for detection of skull base invasion [25]. Figure 4 shows post-operative planning CT and gadolinium-enhanced T1-weighted MRI from a patient with a partially resected nasopharyngeal adenoid cystic cancer. The images illustrate improved tumor delineation, as well as base of skull and perineural extensions.

Lastly, use of MRI is particularly beneficial in patients presenting dental artifacts. Dental artifacts are a common problem in HNC RT planning, given that poor dentition shares risk factors with HNC. High attenuation metal objects[1] such as dental restorations, surgical plates or pins can cause significant scatter artifacts and, as a consequence, can severely impair CT-based oral cavity or oropharynx primary tumor delineation [26]. Variations in magnetic field strength at the interface between dental material and soft tissues can also cause artifacts, but image quality is affected to a lesser extent [27]. Figure 5 shows planning CT and gadolinium-enhanced T1-weighted MRI (modified metal artifact protocol) from a patient with a T4N0 squamous cell cancer of the oropharynx. While the primary lesion is poorly visualized on planning CT, MRI shows a well-defined right oropharynx lesion measuring 4.4 cm with extension to the median pterygoid muscle, buccal space, soft palate, and uvula.

In conclusion, the use of MRI has become an essential part of HNC RT planning owing to the increased accuracy of co-registration with planning CT and improved tumor and organs at risk delineation, particularly for oral cavity, oropharynx, and skull base sites. However, planning MRI

[1] The MRI restrictions (if any) of the metal implant must be considered prior to patient undergoing MRI exam. MR imaging of patients with metallic implants brings specific risks. However, certain implants are approved by the governing regulatory bodies to be MR conditionally safe. For such implants, the previously mentioned warning may not be applicable. Please contact the implant manufacturer for the specific conditional information. The conditions for MR safety are the responsibility of the implant manufacturer, not of Siemens Healthcare.

Figure 4: Improved assessment of soft tissue, base of skull, and perineural invasion in a case of nasopharynx adenoid cystic cancer.

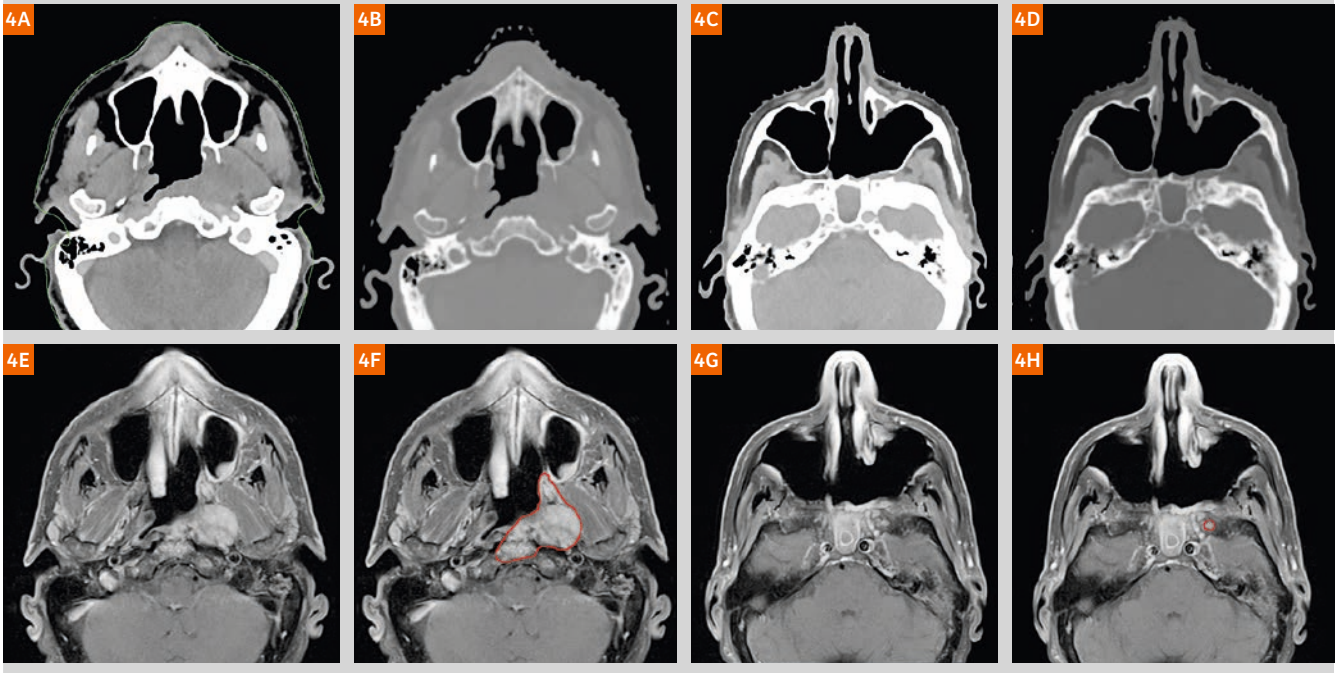

This patient presented with a left T4N0 adenoid cystic cancer of the nasopharynx with cranial nerve involvement and positive biopsy at the clivus, status post partial resection. Planning CT **(4A, B)** shows a post-operative left parapharyngeal residual lesion; gadolinium-enhanced T1-weighted MRI allows to better appreciate extensions to the retropharynx, medial and lateral pterygoid plates, and clivus **(4E, F),** as well as perineural dissemination along extracranial V3 path **(4G, H).**

Figure 5: MRI improves oropharyngeal tumor delineation in a patient with important artifacts secondary to dental amalgams.

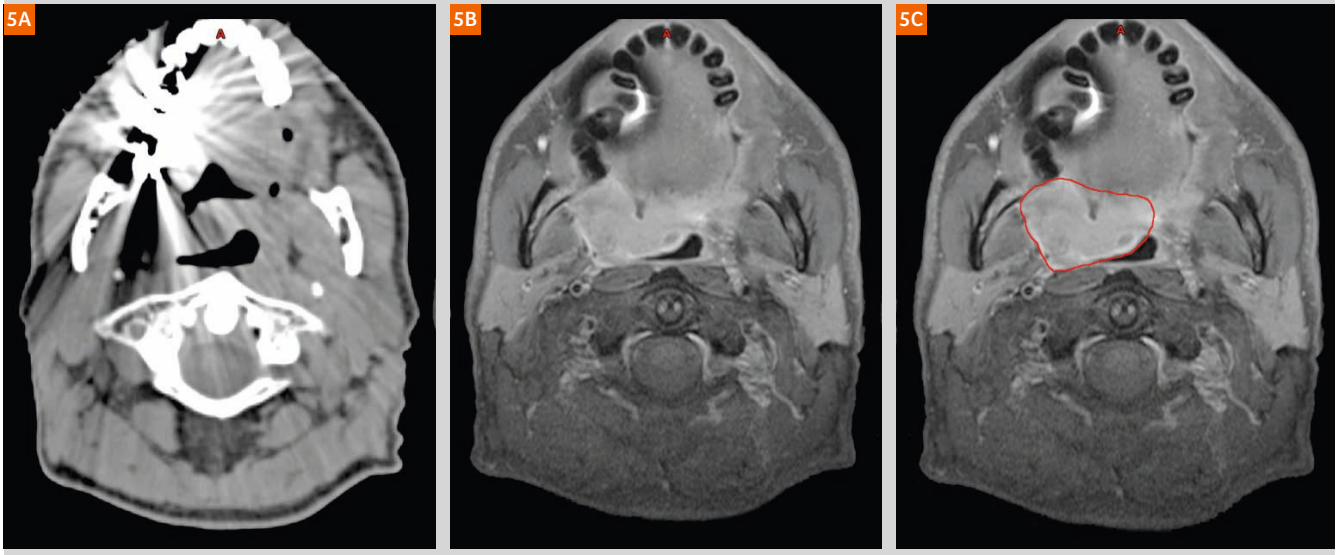

This patient presented with a right T4N0 squamous cell cancer of the oropharynx that can hardly be seen on planning CT due to important dental artifacts **(5A);** on T1-weighted MRI, a well delineated 4.4 cm oropharynx lesion, invading the right median pterygoid muscle, joining the right buccal space and extending to the soft palate and uvula is demonstrated **(5C, D).**

remains associated with several challenges including the management of geometric distortions, the need for MRI compatible immobilisation devices that maintain image-quality, the prolonged time of acquisition, and the increased use of resources. In addition, there remains uncertainty as to which imaging modality is closest to ground-truth. Considering the low concordance between CT-, FDG-PET-, and MRI-based delineations [22], MRI currently remains a complementary imaging modality to be used in combination with FDG-PET and physical examination for safe target volume delineation. Synthetic CT solutions, deriving relative electronic density data from MRI imaging, are currently being evaluated at the CHUM and, in the upcoming years, will likely lead to a more widespread adoption of MR-based workflow in HNC [28–31]. In addition, the potential value of functional MRI in HNC radiotherapy for predicting tumor response and spatiotemporal mapping of radioresistant tumor areas is currently under investigation [25, 32–35]. With the emergence of more robust data on functional imaging biomarkers, diffusion-weighted and dynamic contrast-enhanced MRI may become crucial tools to the promising avenues of dose painting and adaptive radiotherapy.

References

1 Ahmed M, Schmidt M, Sohaib A, Kong C, Burke K, Richardson C, et al. The value of magnetic resonance imaging in target volume delineation of base of tongue tumours--a study using flexible surface coils. Radiotherapy and oncology : journal of the European Society for Therapeutic Radiology and Oncology. 2010;94(2):161-7.

2 Khoo VS, Joon DL. New developments in MRI for target volume delineation in radiotherapy. The British journal of radiology. 2006;79 Spec No 1:S2-15.

3 Dirix P, Haustermans K, Vandecaveye V. The value of magnetic resonance imaging for radiotherapy planning. Seminars in radiation oncology. 2014;24(3):151-9.

4 Paulson ES, Erickson B, Schultz C, Allen Li X. Comprehensive MRI simulation methodology using a dedicated MRI scanner in radiation oncology for external beam radiation treatment planning. Medical physics. 2015;42(1):28-39.

5 Schmidt MA, Payne GS. Radiotherapy planning using MRI. Physics in medicine and biology. 2015;60(22):R323-61.

6 Metcalfe P, Liney GP, Holloway L, Walker A, Barton M, Delaney GP, et al. The potential for an enhanced role for MRI in radiation-therapy treatment planning. Technology in cancer research & treatment. 2013;12(5):429-46.

7 Prestwich RJ, Sykes J, Carey B, Sen M, Dyker KE, Scarsbrook AF. Improving target definition for head and neck radiotherapy: a place for magnetic resonance imaging and 18-fluoride fluorodeoxyglucose positron emission tomography? Clinical oncology (Royal College of Radiologists (Great Britain)). 2012;24(8):577-89.

8 Hanvey S, McJury M, Tho LM, Glegg M, Thomson M, Grose D, et al. The influence of MRI scan position on patients with oropharyngeal cancer undergoing radical radiotherapy. Radiation oncology (London, England). 2013;8:129.

9 Chung NN, Ting LL, Hsu WC, Lui LT, Wang PM. Impact of magnetic resonance imaging versus CT on nasopharyngeal carcinoma: primary tumor target delineation for radiotherapy. Head & neck. 2004;26(3):241-6.

10 Weber AL, Romo L, Hashmi S. Malignant tumors of the oral cavity and oropharynx: clinical, pathologic, and radiologic evaluation. Neuroimaging clinics of North America. 2003;13(3):443-64.

11 Emami B, Sethi A, Petruzzelli GJ. Influence of MRI on target volume delineation and IMRT planning in nasopharyngeal carcinoma.

International journal of radiation oncology, biology, physics. 2003;57(2):481-8.
12 O'Daniel JC, Rosenthal DI, Garden AS, Barker JL, Ahamad A, Ang KK, et al. The effect of dental artifacts, contrast media, and experience on interobserver contouring variations in head and neck anatomy. American journal of clinical oncology. 2007;30(2):191-8.
13 Tien RD, Robbins KT. Correlation of clinical, surgical, pathologic, and MR fat suppression results for head and neck cancer. Head & neck. 1992;14(4):278-84.
14 Phillips CD, Gay SB, Newton RL, Levine PA. Gadolinium-enhanced MRI of tumors of the head and neck. Head & neck. 1990;12(4):308-15.
15 Rasch C, Keus R, Pameijer FA, Koops W, de Ru V, Muller S, et al. The potential impact of CT-MRI matching on tumor volume delineation in advanced head and neck cancer. International journal of radiation oncology, biology, physics. 1997;39(4):841-8.
16 Bird D, Scarsbrook AF, Sykes J, Ramasamy S, Subesinghe M, Carey B, et al. Multimodality imaging with CT, MR and FDG-PET for radiotherapy target volume delineation in oropharyngeal squamous cell carcinoma. BMC cancer. 2015;15:844.
17 Rasch C, Steenbakkers R, van Herk M. Target definition in prostate, head, and neck. Seminars in radiation oncology. 2005;15(3):136-45.
18 Brouwer CL, Steenbakkers RJ, Bourhis J, Budach W, Grau C, Gregoire V, et al. CT-based delineation of organs at risk in the head and neck region: DAHANCA, EORTC, GORTEC, HKNPCSG, NCIC CTG, NCRI, NRG Oncology and TROG consensus guidelines. Radiotherapy and oncology: journal of the European Society for Therapeutic Radiology and Oncology. 2015;117(1):83-90.
19 Liao LJ, Lo WC, Hsu WL, Wang CT, Lai MS. Detection of cervical lymph node metastasis in head and neck cancer patients with clinically N0 neck-a meta-analysis comparing different imaging modalities. BMC cancer. 2012;12:236.
20 Sun J, Li B, Li CJ, Li Y, Su F, Gao QH, et al. Computed tomography versus magnetic resonance imaging for diagnosing cervical lymph node metastasis of head and neck cancer: a systematic review and meta-analysis. OncoTargets and therapy. 2015;8:1291-313.
21 Kato H, Kanematsu M, Watanabe H, Mizuta K, Aoki M. Metastatic retropharyngeal lymph nodes: comparison of CT and MR imaging for diagnostic accuracy. European journal of radiology. 2014;83(7):1157-62.
22 Thiagarajan A, Caria N, Schoder H, Iyer NG, Wolden S, Wong RJ, et al. Target volume delineation in oropharyngeal cancer: impact of PET, MRI, and physical examination. International journal of radiation oncology, biology, physics. 2012;83(1):220-7.
23 Gandhi D, Gujar S, Mukherji SK. Magnetic resonance imaging of perineural spread of head and neck malignancies. Topics in magnetic resonance imaging: TMRI. 2004;15(2):79-85.
24 Geets X, Daisne JF, Arcangeli S, Coche E, De Poel M, Duprez T, et al. Inter-observer variability in the delineation of pharyngo-laryngeal tumor, parotid glands and cervical spinal cord: comparison between CT-scan and MRI. Radiotherapy and oncology: journal of the European Society for Therapeutic Radiology and Oncology. 2005;77(1):25-31.
25 Zhang SX, Han PH, Zhang GQ, Wang RH, Ge YB, Ren ZG, et al. Comparison of SPECT/CT, MRI and CT in diagnosis of skull base bone invasion in nasopharyngeal carcinoma. Bio-medical materials and engineering. 2014;24(1):1117-24.
26 Cooper JS, Mukherji SK, Toledano AY, Beldon C, Schmalfuss IM, Amdur R, et al. An evaluation of the variability of tumor-shape definition derived by experienced observers from CT images of supraglottic carcinomas (ACRIN protocol 6658). International journal of radiation oncology, biology, physics. 2007;67(4):972-5.
27 Klinke T, Daboul A, Maron J, Gredes T, Puls R, Jaghsi A, et al. Artifacts in magnetic resonance imaging and computed tomography caused by dental materials. PloS one. 2012;7(2):e31766.
28 Korhonen J, Kapanen M, Keyrilainen J, Seppala T, Tuomikoski L, Tenhunen M. Influence of MRI-based bone outline definition errors on external radiotherapy dose calculation accuracy in heterogeneous pseudo-CT images of prostate cancer patients. Acta oncologica (Stockholm, Sweden). 2014;53(8):1100-6.
29 Korhonen J, Kapanen M, Keyrilainen J, Seppala T, Tenhunen M. A dual model HU conversion from MRI intensity values within and outside of bone segment for MRI-based radiotherapy treatment planning of prostate cancer. Medical physics. 2014;41(1):011704.
30 Gudur MS, Hara W, Le QT, Wang L, Xing L, Li R. A unifying probabilistic Bayesian approach to derive electron density from MRI for radiation therapy treatment planning. Physics in medicine and biology. 2014;59(21):6595-606.
31 Hsu SH, Cao Y, Huang K, Feng M, Balter JM. Investigation of a method for generating synthetic CT models from MRI scans of the head and neck for radiation therapy. Physics in medicine and biology. 2013;58(23):8419-35.
32 Quon H, Brizel DM. Predictive and prognostic role of functional imaging of head and neck squamous cell carcinomas. Seminars in radiation oncology. 2012;22(3):220-32.
33 Vandecaveye V, De Keyzer F, Nuyts S, Deraedt K, Dirix P, Hamaekers P, et al. Detection of head and neck squamous cell carcinoma with diffusion weighted MRI after (chemo)radiotherapy: correlation between radiologic and histopathologic findings. International journal of radiation oncology, biology, physics. 2007;67(4):960-71.
34 Wang H, Balter J, Cao Y. Patient-induced susceptibility effect on geometric distortion of clinical brain MRI for radiation treatment planning on a 3T scanner. Physics in medicine and biology. 2013;58(3):465-77.
35 Powell C, Schmidt M, Borri M, Koh DM, Partridge M, Riddell A, et al. Changes in functional imaging parameters following induction chemotherapy have important implications for individualised patient-based treatment regimens for advanced head and neck cancer. Radiotherapy and oncology: journal of the European Society for Therapeutic Radiology and Oncology. 2013;106(1):112-7.

Contact

Houda Bahig, M.D.
Radiation Oncologist

Centre Hospitalier de l'Université de Montréal
1560 Sherbrooke Street East
H2L 4M1
Montreal, QC
Canada
houda.bahig.chum@ssss.gouv.qc.ca